International Journal of Computer Information Systems and Industrial Management Applications
ISSN 2150-7988 Volume 3 (2011) pp.150-158

Skull Stripping Magnetic Resonance Images Brain Images: Region Growing versus Mathematical Morphology

Rosniza Roslan[1], Nursuriati Jamil[2] and Rozi Mahmud[3]

[1] Faculty of Computer & Mathematical Sciences,
Universiti Teknologi MARA, 40450 Shah Alam, Selangor, Malaysia.
rrosnisz@yahoo.com

[2] Faculty of Computer & Mathematical Sciences,
Universiti Teknologi MARA, 40450 Shah Alam, Selangor, Malaysia.
liza@tmsk.uitm.edu.my

[3] Faculty of Medicine and Health Sciences,
Universiti Putra Malaysia, 43400 Serdang, Selangor, Malaysia.
rozi@medic.upm.edu.my

***Abstract*: Skull stripping is a major phase in MRI brain imaging applications and it refers to the removal of the brain's non-cerebral tissues. The main problem in skull-stripping is the segmentation of the non-cerebral and the intracranial tissues due to their homogeneity intensities. Numerous techniques were applied in the studies of skull stripping, most common are region growing and mathematical morphology. This paper investigated the strength and weaknesses of these two methods on three types of MRI brain images. Unlike previous researches which normally tested on one type of MRI images only, this paper experimented on ninety samples of T1-weighted, T2-weighted and FLAIR MRI brain images. Qualitative evaluations showed that skull stripping using mathematical morphology outperformed region growing at an acceptance rate of 95.5%, whereas quantitative evaluation using Area Overlap, False Positive Rate and False Negative Rate produced of 96.2%, 2.2% and 1.6% respectively.**

***Keywords*: Skull Stripping, Mathematical Morphology, Region Growing, MRI, Thresholding**

I. Introduction

Brain imaging has been widely used in many medical applications that are helpful in the detection of brain abnormalities such as brain tumour, stroke, paralysis and breathing difficulties. Over the decades, skull stripping has been one of the major pre-processing phases in brain imaging applications [1] and for further analysis of Magnetic Resonance Imaging (MRI) brain images [2]. Previous studies involving MRI brain images and skull stripping used in clinical applications are brain mapping [3], brain tumour volume analysis [4], tissue classification [5], epilepsy analysis [6] - [8] and brain tumour segmentation [9] [27]. MRI brain images are utilized in this paper as the soft tissues are easily manipulated and offers higher-definition images compared to the others [10] [11], thus is helpful in diagnosing some brain irregularities [2].

Skull stripping is a major phase in brain imaging applications [1] and it refers to the removal of non-cerebral tissues such as skull, scalp, vein or meninges [1]. Numerous techniques have been applied in skull stripping studies, most common are region growing techniques [14] [15] [2] and mathematical morphology [5] [16] [17] [18] [19] [24] [25].

Region growing works by appending neighbouring pixels of starting seed pixel to form a region based on predefined criteria [15] [20]. The region grows by appending to each seed pixel those neighbouring pixels that have the similar properties to the seed point such as specific range of gray level values or colour. The disadvantage of this algorithm is that user has to select the seed regions [14] and threshold values [2]. Therefore, Park et al. [2] addressed this problem by introducing a 2D region growing algorithm that automatically selects seed regions that correspond to the brain and non-brain regions. Thus, it is robust against low contrast, noise, intensity inhomogeneities and effectively addresses the connection issue of the brain regions.

Gonzales & Woods [20] defined mathematical morphology as a tool for extracting image components useful in the representation and description of region shape such as boundaries, skeletons and convex hull. Previous studies of brain segmentation and analysis have employed mathematical morphology [5] [16] [17] [18] [19]. These studies commonly used morphological opening to separate the brain tissues from the surrounding tissues as well as morphological dilation and closing are required for the segmentation of the brain tissues without holes. As morphological operations requires binary form images, it provides a simple and efficient way for integrating distance, neighbourhood information in segmentation [16] as well as offers a unified and powerful approach to numerous image processing problems [20]. However, morphology requires a prior binarization of the image into object and background regions [16].

Thresholding creates binary images from gray-level ones by turning all pixels below of the threshold value to zero and all pixels above the threshold value to one [21]. The selection of an adequate threshold of gray-level for extracting objects from their background is important [22] [26] and thresholding algorithm is an intuitive properties and simplicity of implementation of the application of image segmentation [20]. However, it is difficult to find the robust threshold values which produce a good output for some of the images [24]. The mathematical morphology segmentation using double thresholding produced more robust and accurate skull-stripping compared to Otsu's thresholding as proposed in [24]. Therefore, this paper proposed utilizing double threshold values during skull stripping using mathematical morphology to address the drawback of choosing the incorrect threshold values. The proposed thresholding technique is then compared to the popular Otsu's thresholding in performing skull stripping as well as region growing technique by using the double and Otsu threshold values.

II. Methodology

As mentioned previously, this paper investigated the performance of two most popular methods of skull stripping that is mathematical morphology and region growing. The first part of the experiment addressed the issue of identifying the threshold value used in performing skull stripping using mathematical morphology. **Figure 1** shows the process flow of the proposed algorithms.

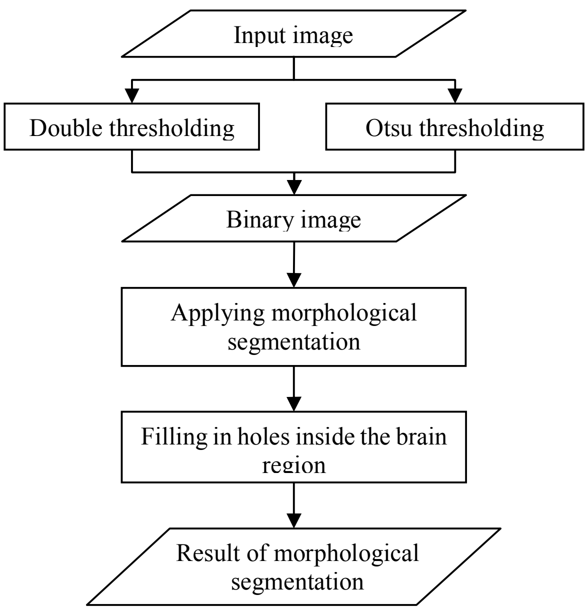

Figure 1. Process flow of the proposed mathematical morphology method

The second part of the experiment compared the performance of region growing against mathematical morphology in performing skull stripping. The same set of data is used and both qualitative and quantitative measurements are conducted to compare the performance of both methods. Region growing's process flow is illustrated in **Figure 2**. In the next sections of methodology, each phase of the process flow is further explained.

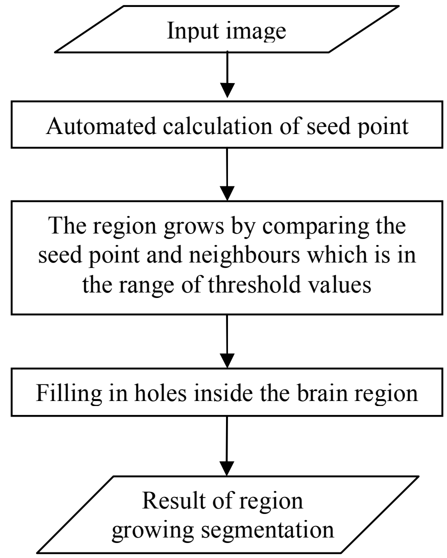

Figure 2. Process flow of the proposed region growing method

A. Data Collections

Two-dimensional MRI data sets are collected from the Hospital Sungai Buloh in Selangor. A total of 90 MRI brain images for all image sequences are utilized as the test images. The data sets were obtained from adults ranging from 18 to 60 years old. Details of image sequences used in the experiments are:

- T1-Weighted of axial orientation (30 images)
- T2-Weighted of axial orientation (30 images)
- Fluid Attenuated Inversion Recovery (FLAIR) of axial orientation (30 images)

B. Thresholding

Two thresholding methods are experimented for skull stripping using mathematical morphology that is double thresholding and Otsu's method. The purpose of this experiment is to identify the robust threshold values to remove the non-cerebral tissue from MRI brain images. **Figure 3** illustrates the non-cerebral tissues (skull, cerebrospinal fluid, meninges) to be extracted.

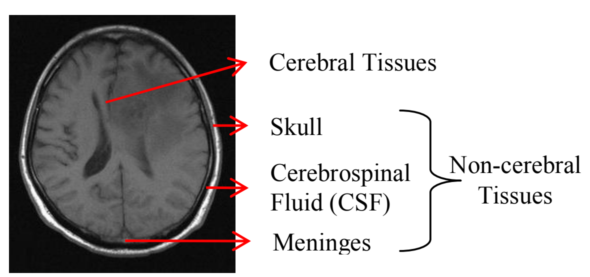

Figure 3. Anatomical of cerebral and non-cerebral tissues

1) Double thresholding

The selection of the double threshold values means choosing on the dual threshold values which defines the intensities of the non-cerebral tissues (i.e. skull, cerebrospinal fluid, meninges) of all 90 MRI images. **Table 1** tabulated the results.

Table 1. Average intensities of cerebral and non-cerebral tissues

Non-cerebral Tissue	Average Intensities
Skull	0.70-1.00
CSF	0.00-0.20
Meninges	0.15-0.50
Cerebral Tissues	0.2-1.0

As can be seen from **Table 1**, the average intensities of the non-cerebral tissues are within the range of 0 to 0.5 and 0.7 to 1.0. For instance in **Figure 4**, the lower intensity referred to 20% of the cumulative histogram constituting mostly the background and CSF. Whereas the upper intensity which lies above 0.7 of intensity histogram is the skull since they generally appeared brighter than other non-cerebral tissue. Thus, the binary image, *g(x, y)* of the original image, *f(x, y)* using the double threshold values can be defined as follows.

$$g(x,y)=\begin{cases}1;0.2\le f(x,y)\le 0.7\\0\end{cases}$$

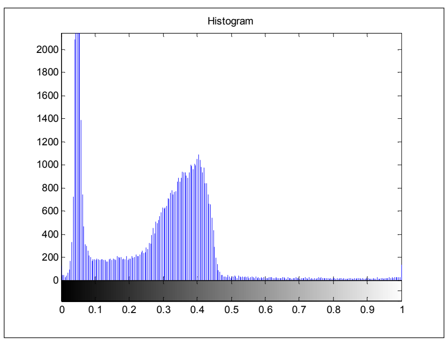

Figure 4. Histogram-based double threshold values estimation

2) Otsu's thresholding

The popular Otsu's [22] algorithm is very simple, utilizing only the zeroth- and the first-order cumulative moments of the gray-level histogram.

$$p_i=\frac{n_i}{N}, p_i\ge 0, \sum_{i=1}^{L}p_i=1$$

An optimal threshold is determined by discriminant criterion which is to maximize the separability of the resultant classes in gray levels. This thresholding method is based on selecting the lowest point between two classes. Therefore, the optimal threshold k^* is defined as:

$$\sigma_B{}^2(k^*)=\max_{1\le k\le L}\sigma_B{}^2(k)$$

and the range of k over the maximum can be restricted to:

$$S^*=\{k;\omega_0\omega_1=\omega(k)[1-\omega(k)]>0, \text{ or } 0<\omega(k)<1\}$$

C. Mathematical Morphology Segmentation

Next, mathematical morphology operations (i.e. erosion, dilation and region filling) are applied to the binary image to remove the non-cerebral tissue. The concept is to convolve the binary image with a structuring element to produce the skull-stripped image. Since the brain is an oval-shape image, a disk-shape structuring element as shown in **Figure 5** is chosen in the convolution process.

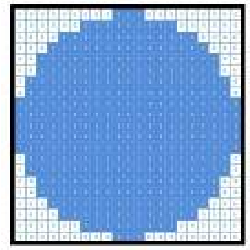

Figure 5. Structuring element of morphological erosion and dilation

Erosion is used to remove the pixels on the MRI brain image's boundaries, thus removing the non-brain regions such as skull, cerebrospinal fluid and meninges. As defined in [20], erosion of binary image, *A* using structuring element, *B* can be denoted as:

$$A\ominus B=\{z|(B)_z\subseteq A\}$$

This equation indicates that the erosion of A by B is the set of all points z such that B, translated by z, is contained in A.

In this proposed algorithm, the morphological dilation is applied in order to enhance and connect all the intracranial tissues within the image. Mathematical morphology dilation [20] of binary image, *A* using the structuring element, *B* in **Figure 5** but with a different size can be denoted as:

$$A\oplus B=\{z\,|\,(\hat{B})_z\cap A\ne\phi\}$$

where ϕ is the empty set. This equation is based on obtaining the reflection of *B* about its origin and shifting this reflection by *z*. The dilation of *A* by *B* then is the set of all displacements, *z* such that $\hat{B}$ and *A* overlap by at least one element.

D. Region Growing

Region growing is a procedure that group pixels into larger regions based on predefined criteria and it started growing with the selected seed point. The segmentation by region growing worked by appending neighbouring pixels of a seed point that was automatically selected based on the centre point of the maximum region area of the axial MRI image.

1) Seed point selection

The seed point is selected by choosing the centre point of the maximum region area within the brain image. For example, **Figure 6** below shows the blue point selected as the seed point of the image.

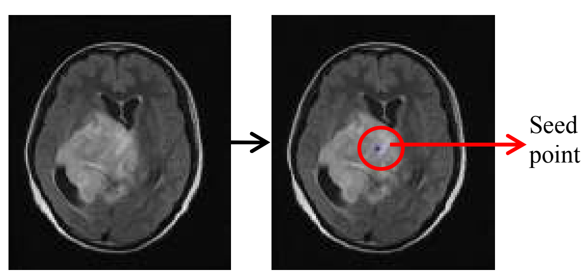

Figure 6. Seed point selection

2) Growing predicates and stopping criteria

The region grew by comparing all 8-neighbouring pixels of the original image with the seed point which is within the range of defined threshold values. The region stopped if the neighbouring pixels are outside the range of the threshold values. The threshold values applied using the double threshold defined in the double thresholding section.

E. Binary Morphological Enhancement

The final step of both mathematical morphology and region growing is an optional process to enhance the appearance of the skull-stripped brain image as shown in **Figure 8** Region filling is used to fill in holes inside the brain region. Given a brain region, A and an initial point p of the holes region, region filling is done using the following equation: $X_k = (X_{k-1} \oplus B) \cap A^C; k = 1,2,3,\ldots$ where $X_0 = p$ and B is a structuring element as shown in **Figure 7**. This process terminates at iteration step k if $X_k = X_{k-1}$.

0	1	0
1	1	1
0	1	0

Figure 7. Structuring element of morphological region filling

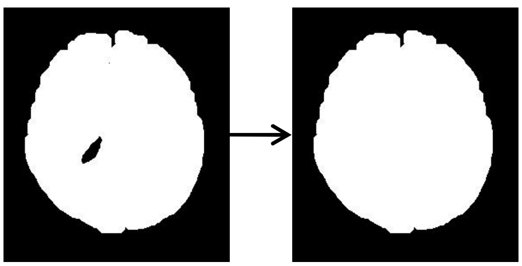

Figure 8. The process of before and after region filling

III. Results and Evaluation

Both region growing and mathematical morphological methods of skull-stripping ware evaluated on 90 MRI brain images of T1-weighted, T2-weighted and FLAIR of axial orientation. The experimented results of the skull-stripped images are evaluated using qualitative visual inspection by expert radiologists, and quantitative evaluation using Area Overlap (AO) [23], False Positive Rate (FPR) [2] and False Negative Rate (FNR) [2].

A. Experiment 1

The first part of the experiment was to compare double thresholding against Otsu's thresholding in determining a more robust threshold values. The visual inspection results of skull-stripping using mathematical morphology on T1-weighted, T2-weighted and FLAIR images are tabulated as shown in **Table 2**.

Table 2. Visual inspection for T1-Weighted, T2-Weighted and FLAIR images using Mathematical Morphology

Data Set		Accept (%)	Reject (%)
T1-Weighted	**Double**	93.3333	6.6667
	Otsu	76.6667	23.3333
T2-Weighted	**Double**	96.6667	3.3333
	Otsu	93.3333	6.6667
FLAIR	**Double**	96.6667	3.3333
	Otsu	93.3333	6.6667

Table 2 shows that skull stripping using double thresholding produced higher acceptance rate compared to Otsu's thresholding for all three types of image sequences. For example, the acceptance rate for skull-stripped T1-weighted images using double thresholding is 16% higher than using Otsu's thresholding.

The quantitative performance evaluation using AO, FPR and FNR of T1-weighted, T2-weighted and FLAIR images are calculated as shown in **Table 3**, **Table 4** and **Table 5** respectively. Prior to evaluations, ground truth data of all 90 skull-stripped images are created by radiologists as benchmark for quantitative evaluations. AO is used to compute the area of intracranial tissues that the proposed algorithms could capture and this method can be considered as a good representation for segmenting the area of intracranial tissues accurately [23]. AO is computed as follows:

$$AO = 100 \times \frac{|S_1 \cap S_2|}{|S_1 \cup S_2|}$$

FPR method is used to quantify the over-segmentation of non-cerebral tissues while FNR method measured the under-segmentation of intracranial tissues within the images. The evaluations are computed as follows:

$$FPR = 100 \times \frac{|S_1 \cap S_2^{\,C}|}{|S_1 \cup S_2|}$$

$$FNR = 100 \times \frac{|S_1^{\,C} \cap S_2|}{|S_1 \cup S_2|}$$

where S_1 represents the area of the skull-stripped images obtained by the proposed algorithms, $S_1^{\,C}$ is the complement of S_1, S_2 represents the area of the ground truth data and $S_2^{\,C}$ is the complement of S_2

Table 3. Mean percentage of Area Overlap T1-Weighted, T2-Weighted and FLAIR images

Data Set	AO (%) Double Threshold	Otsu Threshold
T1-Weighted	95.0879	92.9424
T2-Weighted	97.0903	97.0828
FLAIR	96.4646	96.2163
Average	96.2143	95.4138

As shown in the **Table 3**, average overlap area is higher using double thresholding compared to Otsu's. This indicated that more intracranial tissues are extracted. Thus, the double thresholding are robust against Otsu's for all tested images.

Table 4. Mean percentage of False Positive Rate T1-Weighted, T2-Weighted and FLAIR images

Data Set	FPR (%) Double Threshold	Otsu Threshold
T1-Weighted	2.0626	2.2239
T2-Weighted	2.2775	2.1702
FLAIR	2.1424	1.6142
Average	2.1608	2.0028

Table 4 tabulated the false positive rate and results showed that for T1-weighted images, double thresholding performed better than Otsu's. However, for T2-weighted and FLAIR images, FPR is slightly higher when using double thresholding. This indicates that oversegmentation occurred more when using double thresholding on both T2-weighted and FLAIR images. The main reason is due to the homogeneous intensities of meninges with intracranial tissues as demonstrated in **Figure 9**.

Figure 9. Non-cerebral tissues of meninges

For false negative rate as shown in **Table 5**, skull-stripping using double thresholding again outperformed Otsu's thresholding. As an example, Otsu's thresholding FNR for T1-weighted images is much higher compared to double thresholding. This indicated that Otsu's thresholding tends to undersegment the intracranial tissue. The same undersegmentation occurred for T2-weighted and FLAIR images. Since the AO rate of double thresholding produced more than 95% accuracy as well as its FPR and FNR low error rates of less than 10%, the double thresholding is more robust for all the image sequences.

Figure 10 demonstrated examples of skull-stripped images of mathematical morphology for T1-weighted, T2-weighted and FLAIR image sequences.

Table 5. Mean percentage of False Negative Rate T1-Weighted, T2-Weighted and FLAIR images

Data Set	FNR (%) Double Threshold	Otsu Threshold
T1-Weighted	2.8495	4.8337
T2-Weighted	0.6322	0.7470
FLAIR	1.3930	2.1695
Average	1.6249	2.5834

As double thresholding proved to outperform Otsu's thresholding, the results of skull stripping using double thresholding is used to be evaluated against skull stripping using region growing which is presented in the next section.

B. Experiment 2

The purpose of the second experiment is to evaluate the performances of skull stripping using region growing and mathematical morphology. The qualitative visual inspection results of skull-stripping using region growing and mathematical morphology on T1-weighted, T2-weighted and FLAIR images are tabulated in **Table 6**. As can be seen, for each type of MRI image, mathematical morphology clearly surpassed region growing at an average of 95.5% acceptance rate when evaluated by experts.

Table 6. Qualitative evaluation using Region Growing and Mathematical Morphology

Data Set	Region Growing		Mathematical Morphology	
	Accept (%)	Reject (%)	Accept (%)	Reject (%)
T1-Weighted	36.6667	63.3333	93.3333	6.6667
T2-Weighted	86.6667	13.3333	96.6667	3.3333
FLAIR	73.3333	26.6667	96.6667	3.3333
Average	65.5556	34.4444	95.5556	4.4444

The results of quantitative evaluation using area overlap for all T1-weighted, T2-weighted and FLAIR MRI brain images tabulated as in **Table 7**. **Table 7** shows that the results of skull stripping using mathematical morphology produced higher percentage for all three types of images compared to region growing. For instance, the acceptance rate for AO of the skull-stripped T1-weighted images produced 95% which is higher acceptance rate compared to region growing which produced 79% of AO. This indicated that skull stripping using mathematical morphology produced better results for all three types of images.

Table 7. Mean percentage of Area Overlap T1-Weighted, T2-Weighted and FLAIR images using Region Growing and Mathematical Morphology

Data Set	AO (%) Region Growing	Mathematical Morphology
T1-Weighted	78.8764	95.0879
T2-Weighted	93.4437	97.0903
FLAIR	91.4494	96.4646
Average	87.9232	96.2143

Table 8. Mean percentage of False Positive Rate T1-Weighted, T2-Weighted and FLAIR images using Region Growing and Mathematical Morphology

Data Set	FPR (%) Region Growing	Mathematical Morphology
T1-Weighted	16.7044	2.0626
T2-Weighted	4.1151	2.2775
FLAIR	5.6749	2.1424
Average	8.8315	2.1608

Table 8 demonstrates the results of quantitative evaluation using false negative rate for all T1-weighted, T2-weighted and FLAIR MRI brain images. The results of mathematical morphology presented low percentage compared to high percentage of FPR to region growing. This indicated that less oversegmentation occurred for all three types of images using mathematical morphology. Therefore, the mathematical morphology performed better for all three types of images.

Table 9. Mean percentage of False Negative Rate T1-Weighted, T2-Weighted and FLAIR images using Region Growing and Mathematical Morphology

Data Set	FNR (%)	
	Region Growing	**Mathematical Morphology**
T1-Weighted	4.4191	2.8495
T2-Weighted	2.4412	0.6322
FLAIR	2.8757	1.3930
Average	3.2453	1.6249

Table 9 tabulated the skull-stripping quantitative evaluation using false negative rate. The results showed that mathematical morphology outperformed region growing. The error for mathematical morphology is lower compared to region growing for all three types of images. This lower percentage error denoted that mathematical morphology produced less undersegmentation region of skull-stripped images. Thus, it proved that mathematical morphology performed better than region growing as AO rate produced higher percentage, as well as FPR and FNR also have lower error rate for all image sequences.

Figure 10 and **Figure 11** illustrated the samples of skull-stripped images for all image sequences using mathematical morphology and region growing.

IV. Conclusion

The proposed algorithm of mathematical morphology segmentation of MRI brain images has been utilized and mean percentage of AO, FPR and FNR for each image sequences of all T1-weighted, T2-weighted and FLAIR MRI brain images were evaluated against the ground truth data. **Table 3**, **Table 4** and **Table 5** show the results of mean percentage of AO, FPR and FNR of 30 MRI brain images for each image sequences. Overall, mathematical morphology segmentation using double thresholding produced more robust and accurate skull-stripping compared to Otsu's thresholding as illustrated in Higher mean percentages of intracranial tissues are extracted using double thresholding as well as lower rate of oversegmentation and undersegmentation. Furthermore, mathematical morphology segmentation using double thresholding took shorter time to complete the segmentation compared to region growing. **Table 10** illustrated an average execution time of mathematical morphology segmentation and region growing using double thresholding. For example, morphology segmentation took 2 seconds to complete compared to region growing which took 2.5 minutes for T2-weighted images. Thus, skull stripping region growing required high CPU time.

Mathematical morphology has an advantage over region growing since this algorithm only visits the relevant pixels of the image (i.e. $X_k \in A; k = 0,1,2,3,\ldots$ given brain region, A) and less computational compared to region growing. On the other hand, region growing is highly computational since the algorithm requires all neighbouring pixels of the seed points to be visited. Furthermore, region growing also requires the correct selection of seed point and threshold values as different seed point and threshold values will produce different results. Therefore, region growing algorithm is highly dependent on the selection of seed point and threshold values.

Table 10. Execution time of T1-Weighted, T2-Weighted and FLAIR images using Region Growing and Mathematical Morphology

Data Set	Execution Time	
	Region Growing	**Mathematical Morphology**
T1-Weighted	2.5 minutes	2 seconds
T2-Weighted	2.5 minutes	2 seconds
FLAIR	3 minutes	2 seconds
Average	2.67 minutes	2 seconds

Image Sequence	Original Image	Binarization of Double Threshold Values	Morphological of Double Threshold Values	Binarization of Otsu Threshold Values	Morphological of Otsu Threshold Value
T1-Weighted	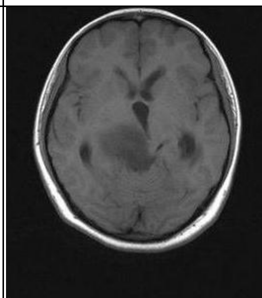	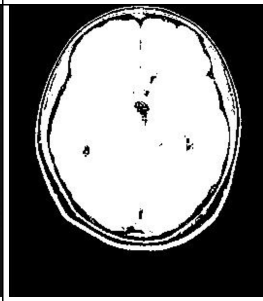	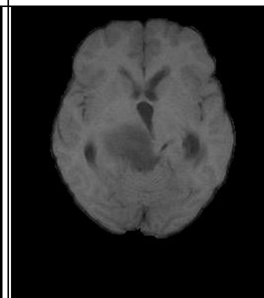		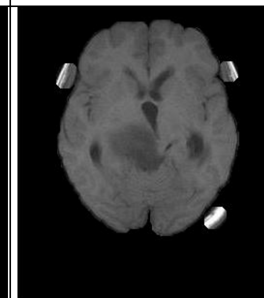
T2-Weighted	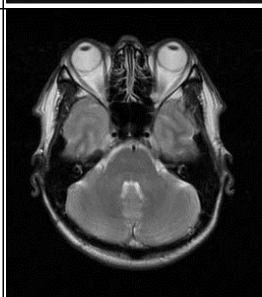	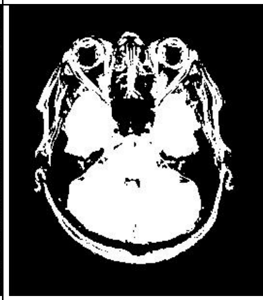	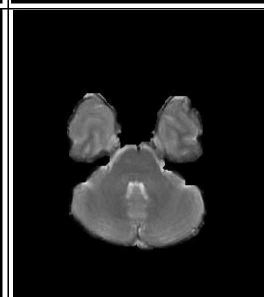	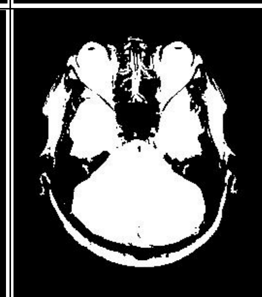	
FLAIR					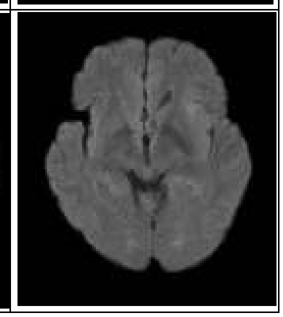

Figure 10. The results of skull-stripped images of the proposed Mathematical Morphology

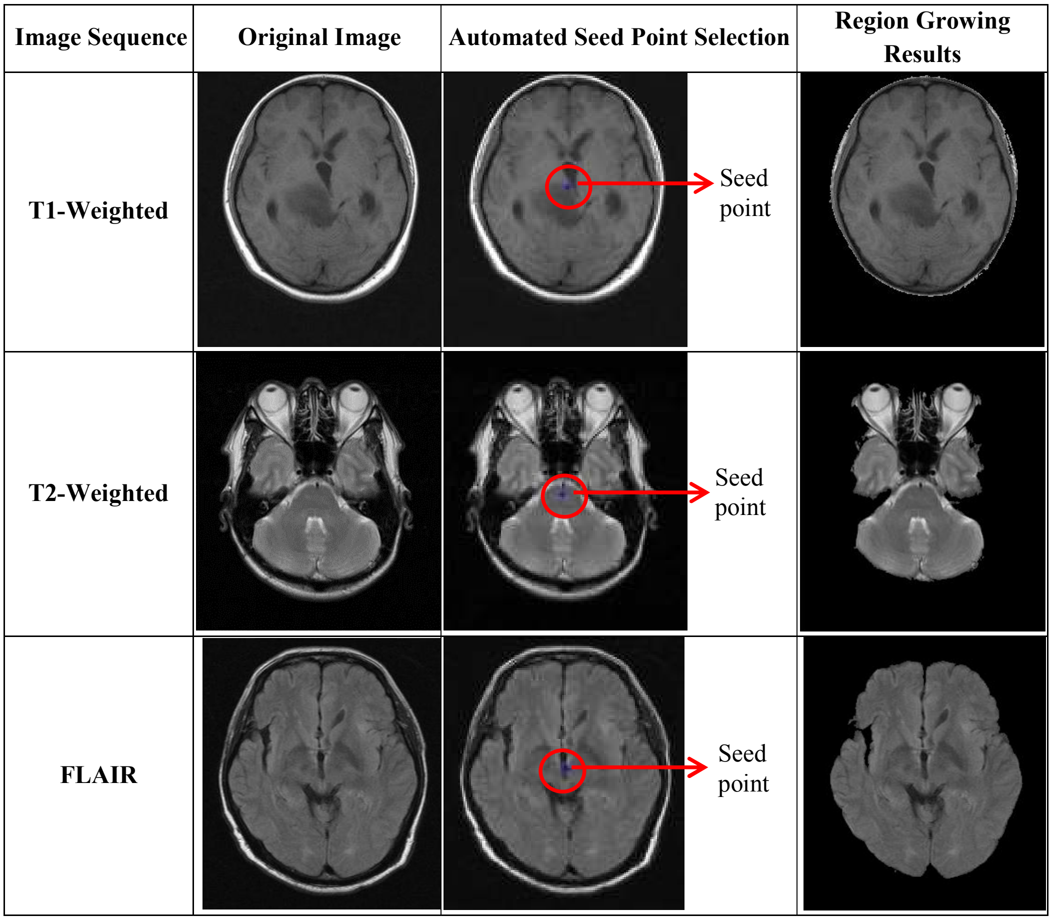

Figure 11. The results of skull-stripped images of the proposed Region Growing

Acknowledgment

This research was supported by the Excellence Fund, Research Management Institute, MARA University of Technology via grant number 600-RMI/ST/DANA 5/3/Dst (243/2009) and the data was collected from Hospital Sungai Buloh, Selangor, Malaysia.

References

[1] H.K. Hahn and H.-O. Peitgen, "The Skull Stripping Problem in MRI Solved by a Single 3D Watershed Transform", *Lecture Notes in Computer Science, Medical Image Computing and Computer-Assisted Intervention (MICCAI),* Vol. 1935/2000, pp. 134-143, 2000.

[2] J.G. Park and C. Lee, "Skull Stripping Based On Region Growing For Magnetic Resonance Brain Images", *NeuroImage,* 47, 1394-1407, 2009.

[3] P. Thompson and A.W. Toga, "A Surface-Based Technique for Warping Three-Dimensional Images of the Brain", *IEEE Transaction Medical Image*, 15, 1996.

[4] R.B. Dubey, M. Hanmandlu and S.K. Gupta, "Region Growing for MRI Brain Tumor Volume Analysis", *Indian Journal of Science and Technology,* Volume 2, No. 9, 2009.

[5] D. Shattuck, S. Sandor-Leahy, K. Schaper, D. Rottenberg and R. Leahy, "Magnetic Resonance Image Tissue Classification using a Partial Volume Model", *Neuroimage,* 13, 856-876, 2001.

[6] K. Jafari-Khouzani, M.R. Siadat, H. Soltanian-Zadeh and K. Elisevich, "Texture Analysis of Hippocampus for Epilepsy", in *Proceedings of SPIE*, Volume 5031, 2003.

[7] K. Jafari-Khouzani, H. Soltanian-Zadeh and K. Elisevich, "Texture analysis of high-resolution FLAIR images for TLE", in *Proceedings of SPIE,* Volume 5747, 2005.

[8] K. Jafari-Khouzani and H. Soltanian-Zadeh, "Hippocampus Volume and Texture Analysis for Temporal Lobe Epilepsy", *IEEE International Conference, Electro/Information Technology*, 394-397, 2006.

[9] N. Moon, E. Bullitt, K. van Leemput and G. Gerig, "Automatic Brain and Tumor Segmentation", *Medical*

Image Computing and Computer-Assisted Intervention, Volume 2488, 2002.
[10] G.B. Chavhan, MRI Made Easy (for Beginners), Jaypee, 2006.
[11] (2009) Tool Module: Brain Imaging. Canadian Institute of Neurosciences, Mental Health and Addiction and Canadian Institute of Research. [Online] Available: http://thebrain.mcgill.ca/flash/capsules/outil_bleu13.html
[12] F. Segonne, A.M. Dale, E. Busa, M. Glessner, D. Salat, H.K. Hahn and B. Fischl, "A hybrid approach to the skull stripping problem in MRI", *NeuroImage*, 22(3), 1060–1075, 2004.
[13] V. Grau, A.U.J. Mewes, M. Alcaniz, R. Kikinis and S.K. Warfield, "Improved watershed transform for medical image segmentation using prior information", *IEEE Trans. Med. Imag.,* 23(4), 447–458, 2004.
[14] R. Adams and L. Bischof, "Seeded region growing", *IEEE Transactions on Pattern Analysis and Machine Intelligence,* Vol. 16(6), 641–646, 1994.
[15] S.A. Hojjatoleslami and J. Kittler, "Region Growing: A New Approach", *IEEE Transactions on Image Processing,* Vol. 7, No. 7, 1998.
[16] T. Kapur, W.E.L. Grimson, W.M. Wells and R. Kikinis, "Segmentation of Brain Tissue from Magnetic Resonance Images", *Medical Image Analysis,* Volume 1, Number 2, pp 109-127, 1996.
[17] M.S. Atkins and B.T. Mackiewich, "Fully Automatic Segmentation of the Brain in MRI", *IEEE Transactions Medical Imaging,* 17(1), 98-107, 1998.
[18] A.F. Goldszal, C. Davatzikos, D.L. Pham, M.X.H. Yan, R.N. Bryan and S.M. Resnick, "An Image Processing System for Qualitative and Quantitative Volumetric Analysis of Brain Images", *Journal Comput. Assist. Tomogr.,* 22(5): 827-837, 1998.
[19] L. Lemieux, G. Hagemann, K. Krakow and F.G. Woermann, "Fast, accurate, and reproducible automatic segmentation of the brain in T1-weighted volume MRI data", *Magnetic Resonance Med.,* 42(1), 127–135, 1999.
[20] R.C. Gonzales and R.E. Woods, *Digital Image Processing,* Second Edition. Prentice Hall, 2002.
[21] B.S. Morse. (2000) Lecture 4: Thresholding. Brigham Young University. [Online]. Available: http://homepages.inf.ed.ac.uk/rbf/CVonline/LOCAL_COPIES/MORSE/threshold.pdf
[22] N. Otsu, "A Threshold Selection Method from Gray-Level Histograms", *IEEE Transactions on Systems, Man, and Cybernetics,* Vol. 9, No. 1, pp. 62-66, Jan 1979.
[23] S.S. Mohamed and M.MA. Salama, "Spectral clustering for TRUS images", *BioMedical Engineering OnLine,* Volume 6, 2007.
[24] R, Roslan, N. Jamil and R. Mahmud, "Skull Stripping of MRI Brain Images using Mathematical Morphology", *IEEE-EBMS Conference on Biomedical Engineering and Sciences (IECBES 2010)*. Nov 2010.
[25] J. Gao and M. Xie, "Skull-stripping MR Brain Images using Anisotropic Diffusion Filtering and Morphological Processing", *IEEE International Symposium on Computer Network and Multimedia Technology,* pp. 1-4, Jan 2009.
[26] M. Azarbad, A. Ebrahimzade and V. Izadian, "Segmentation of Infrared Images and Objectives Detection Using Maximum Entropy Method Based on the Bee Algorithm", *International Journal of Computer Information Systems and Industrial Management Applications (IJCISIM)*, Vol.3 (2011), pp.026-033.
[27] X. Lin, T. Qiu, F. Morain-Nicolier and S. Ruan Automatic Hippocampus Segmentation from Brain MRI Images", *International Journal of Computer Information Systems and Industrial Management Applications (IJCISIM)*, Vol.1 (2009), pp.239-248

Author Biographies

Rosniza Roslan received her bachelor's degree in computational mathematics from Universiti Teknologi MARA, Malaysia in 2009. She is presently a master student at the Universiti Teknologi MARA, Malaysia. Her research interests include image processing and pattern recognition.

Nursuriati Jamil received her Ph. D. in Computer Science from Universiti Kebangsaan Malaysia, Malaysia in 2008. She is currently an Associate Professor at the Faculty of Computer and Mathematical Sciences, Universiti Teknologi MARA, Malaysia. Her research interests include image processing and multimedia information retrieval .She has published numerous papers and refereed journals and conferences on image processing and image retrieval.

Rozi Mahmud received her bachelor of medicine from Universiti Malaya, Malaysia in 1988 and Master in Radiology from Universiti Kebangsaan Malaysia, Malaysia in 1999. She is currently an Associate Professor at the Faculty of Medicine and Health Sciences, Universiti Putra Malaysia. Her field of specialization is general radiology and radiology of female diseases, applied medical informatics, image processing and computer aided diagnosis.